Int. J. Multiphase Flow, Vol. 1, pp. 525–535. Pergamon Press, 1974. Printed in Great Britain.

SURFACE-ATTACHING PROBABILITIES FOR PARTICLES IN A TURBULENT FLAT PLATE BOUNDARY LAYER

J.B. WEDDING* and J.J. STUKEL**

University of Illinois at Urbana-Champaign, Urbana, Illinois (U.S.A.)

(Received November 27, 1973)

Summary

Measurements of the positional variation of surface-attaching probabilities for 6.77μ uncharged monodisperse uranine aerosol particles on a stainless steel plate are presented for a turbulent flat plate boundary layer. The results presented include results for conditions in which the attaching probability is unity and less than unity. It was found that the variation of the attaching probability was invariant with position once the boundary layer became fully turbulent.

Introduction

Turbulent deposition has been studied by numerous researchers including Friedlander [1, 2], Owen [3], Davies [4, 5], Sehmel [6, 7] and Soo [8, 9, 10].

Recently, Soo [10] attacked the problem of deposition in a fully developed turbulent pipe flow by introducing a sticking (attaching) probability for aerosol clouds coming in contact with a surface. Soo [11] noted that the attaching probability is a function of material properties, has a value ranging from 0 to 1, and is a strong function of the adhesive forces between the particle and the surface.

The discussion which follows deals with the problem of determining attaching probabilities for turbulent flow over a flat plate. Total deposition at regular intervals on a flat plate suspended in a wind tunnel are determined for a turbulent boundary layer with low free stream grid-controlled turbulence. From these data, attaching probabilities are determined for a well defined developing boundary layer.

Governing equations

In attempting to solve the equations governing the flow of particles over a

*Research Assistant, Department of Mechanical and Industrial Engineering.
**Associate Professor of Civil Engineering and Mechanical Engineering.

flat plate, the question of appropriate boundary conditions arises. For a given fluid velocity distribution, the momentum and diffusion equations can be solved for the boundary condition of particle velocity at the wall (subscript w).

$$U_{pw} = -L_p \left.\frac{\partial U_p}{\partial x_n}\right|_w + U_{pi} \tag{1}$$

where L_p is the interaction length, x_n is the coordinate normal to the wall, and U_{pi} is the particle velocity at the wall due to the inertia effect. The boundary condition of particle density at the wall is given by:

$$D_p \left.\frac{\partial \rho_p}{\partial x_n}\right|_w = (1-\sigma)\,[(f_{pn})T_s]\,\rho_{pw} - \sigma_w\,(f_w T_s)\rho_{pw} -$$

$$- \,[(1-\sigma)\rho_{pw} - \sigma'_w \rho_{pb}]\;(f_L T_s) + J_s$$

where D_p is the particle diffusivity, ρ_p is the particulate cloud density, ρ_{pw} is the particulate density at the wall, T_s is the relaxation time, f_{pn} is the field forces per unit mass, σ is the attachment probability for deposition, f_w is the surface force per unit mass, σ_w is the attachment probability prior to the build-up of a monolayer of deposited material, f_L is the lift force per unit mass due to fluid shear in the vicinity of the surface, σ'_w is the probability of re-entrainment due to lift forces, ρ_{pb} is the density of the packed bed on the collector, and J_s accounts for the splashing phenomena discussed by Soo [12].

The first term describes the mass flux to the surface due to field forces, the second term gives the deposition due to surface forces, the third term accounts for any erosion of material from a packed bed of particles on the surface due to fluid shear and the last term denotes those particles in a deposited layer which are re-entrained due to large particles hitting smaller particles in the deposited layer thus causing them to be re-entrained into the stream. In this investigation, the experimental conditions were controlled such that the following terms were always negligible:

$$\left[(1-\sigma)\rho_{pw} - \sigma'_w\,\rho_{pb}\right] f_L T_s + J_s$$

In addition, by removing the charge on the aerosol prior to its arrival at the test section such that

$$\sigma_w(f_w \rho_{pw} T_s) >> (1-\sigma)\,(f_{pn})\,\rho_{pw} T_s$$

the conditions at the boundary can be described by

$$J = -D_p \left.\frac{\partial \rho_p}{\partial x_n}\right|_w = \sigma_w\,[f_w \rho_{pw} T_s] \tag{2}$$

A typical condition in which this is valid is when small uncharged particles are deposited on a flat plate. This work deals with the estimation of σ_w for such a case.

Experimental set-up

A one-foot-square steel wind tunnel approximately 24 ft. in length was constructed as a transport system for the deposition studies as is shown in Fig. 1. Air entering the system passed through a 2 ft. × 2 ft. × 1 ft. absolute filter (99.99 % capture efficiency for $D_p > 0.3\mu$) and converged into the one-ft.-square working section. This enabled flow rates up to 1150 cfm (filter capacity) to be achieved, thus allowing velocities of nearly 600 cm/s in the test section. The flow was induced by a blower on the exit end and exhausted through a ventilating hood. The flow rates were easily adjusted by a damper on the blower and were measured by a pressure drop across a calibrated ASME standard nozzle.

Monodisperse uranine particles [13] were produced by a vibrating orifice aerosol generator. A schematic of the aerosol generation system is shown in

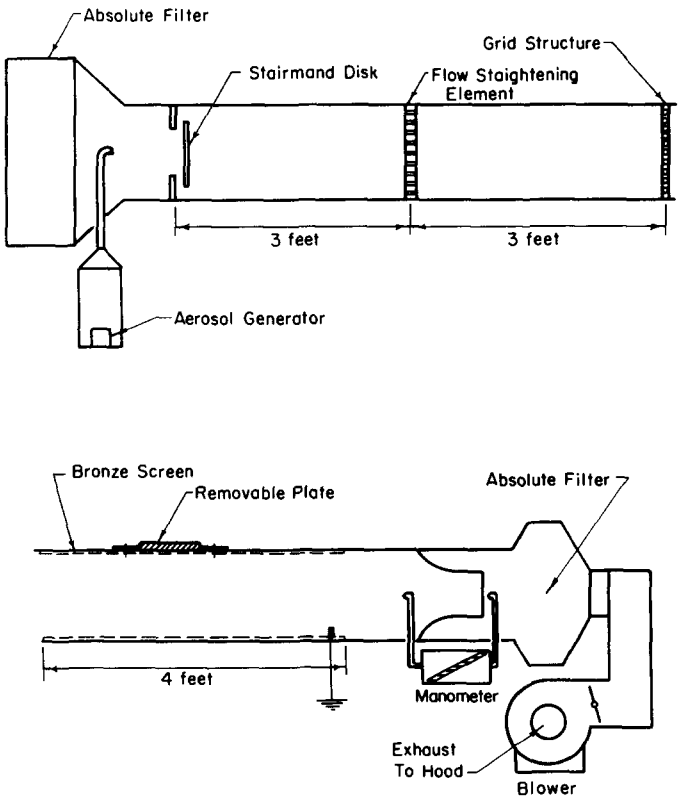

Fig. 1. Experimental configuration.

Fig. 2. The aerosol drying system consisted of an absolute filter (99.99 % capture efficiency for particles greater than 0.3μ diameter) and an air heating section to increase its adsorption capacity for the volatile solvent. The drying air was then passed through a static eliminator (Po 210 source) producing a flow of ionized air to remove any residual charge residing on the particles. The aerosol was introduced as shown in Fig. 1 immediately downstream of the filter in the converging section and parallel to the flow direction through a 90 degree turn in the brass tubing. The flow then passed through a Stairmand Disk [14] to increase mixing and homogeneity of aerosol in the flow stream.

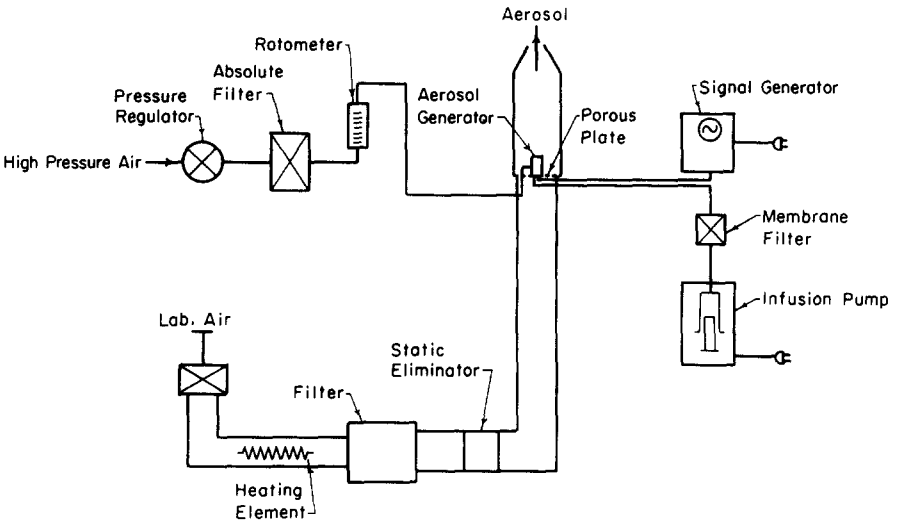

Fig. 2. Monodisperse aerosol generator.

The disk greatly increased the turbulent scale of the airstream. In order to reduce the large scale turbulence, the air was first passed through a plywood grid full of 1 in. diameter holes and then through a series of five 1 ft. × 1 ft. × 1/16 in. mesh grids spaced 1 in. apart [15]. This latter array of screens further reduced the turbulence intensity to 0.8 percent) and produced nearly isotropic turbulence in the test section. The aerosol then entered a 4-ft.-long plexiglass test section equipped with removable elements at the top and side.

The aerosol flux was measured with an isokinetic nozzle—filter arrangement held in place by a thin, vertical rod attached to a traversing mechanism.

The flat plate used for deposition studies was made of stainless steel and was 24 in. × 6 in. × 3/16 in. in dimension. It was suspended in the center of the duct with the leading edge 6 in. (or about 100 mesh diameters) downstream from the grid system. The plate was held in place by 10 rods, 1/16 in. in diameter, threaded into the sides of the plate to isolate it from any wall support effects and to enable it to be electrically grounded. The plate had a rounded-circular nose (1:1 ellipse) to produce laminar separation at the nose

and to reduce the sensitivity of the plate to the angle of attack (although the plate was kept exactly level at all times).

Turbulence intensity and mean velocity profile measurements were made along the flat plate before the addition of any particles into the tunnel with a single channel T.S.I. hot wire anemometer and a boundary layer probe.

Results and Discussion

Carrier gas

A study of the grid-controlled turbulence intensity and the mean velocity profile was undertaken, beginning at a downstream distance from the grid of approximately 100 mesh diameters with the flat plate removed from the test section. The flow velocity was 268 cm/s (8.8 ft./s), yielding a Reynolds number of about 55,000.

$\bar{U}$ readings taken from the entire duct cross-section at 100 mesh diameters downstream (the plane immediately perpendicular to the chosen position for the flat plate) revealed a blunt, square profile of the fluid approaching the plate for nearly an 11-in.-square region. Only the outer inch began to show wall effects and, thus, it was felt that the plate was suspended in a well defined, well controlled turbulent regime allowing a reasonable, reproducible study of the deposition caused by the boundary layer alone.

Hot wire measurements in the boundary layer of the 24 in. × 6 in. flat plate yielded $\bar{U}$ and u' values. Readings were taken 1 in. upstream of the leading edge and at 1 in. intervals along the plate in the downstream (z) direction. Laterally, the entire 6 in. width was analyzed revealing a 4 in. center width unaffected by the plate supporting rods. Thus, deposition analysis excluded the outer 1 in. on each side of the suspended plate. The hot wire analysis results are summarized in Figs. 3 and 4.

These plots reflect the developing nature of the profile. Published shape factor data [16] show that a laminar boundary layer has H values above 2.0, where H is the ratio of the boundary layer displacement thickness and the momentum thickness. The values obtained show H from about 2.5 at x = 6 in. to about 1.7 at x = 23 in. The irregular nature of the turbulent boundary layer and the extreme rate of growth of the redeveloping section is revealed by the nearly constant value of H at x = 10—14 in. Few data are available for Reynolds numbers based on momentum thickness, Re_θ, less than 300, so comparisons are difficult. Data by Hansen [17] suggest that the value of the Reynolds number based on the displacement thickness, Re_δ, for which the boundary layer becomes turbulent is 2700. This corresponds to $H \simeq 2.05$ and $\mathrm{Re}_\theta \simeq 260$.

Curve fitting using data from Robertson [18] enabled a virtual origin of $x_0 = -2.18$ in. to be determined and Reynolds numbers based on $x - x_0$, Re_{x-x_0}, to be calculated.

While a spectrum or intermittency analysis was not undertaken, the anemometer output was continuously monitored with an oscilloscope and

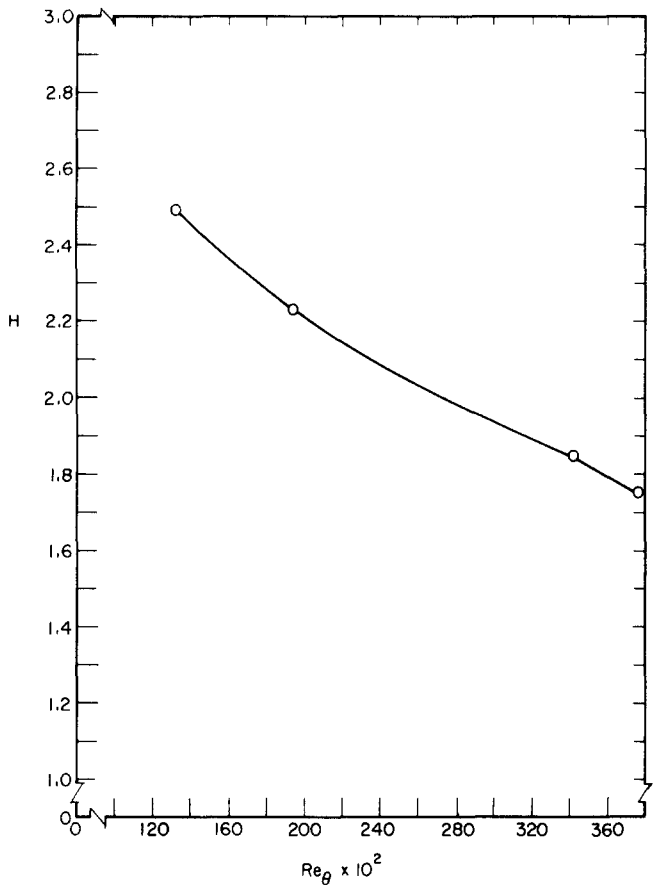

Fig. 3. Measured values of the shape factor H.

the trace was comparable with published oscilloscope velocity traces [19]. The boundary layer appeared fully turbulent (intermittency = 1) from x = 19 in. on *via* oscilloscope traces and the shape factor.

Although spectrum and Reynolds stress measurements were not taken, all the turbulence data recorded were found to be comparable with the measurements of Klebanoff [19] in the fully developed turbulent region.

Particle cloud concentration

The particle concentration profiles were obtained using an isokinetic nozzle sampling system. The samples were taken for a period of 5 min each and the filter paper was analyzed fluorometrically for total mass. The result in micrograms was ratioed to the total volume sampled. The results of the measurements showed that the concentration values at $y = \pm 4$ in. were approximately 85 % of the center value of 3.02 $\mu g/m^3$ and the $y = -2$ in. was on the average 8 % less than the $y = +2$ in. position.

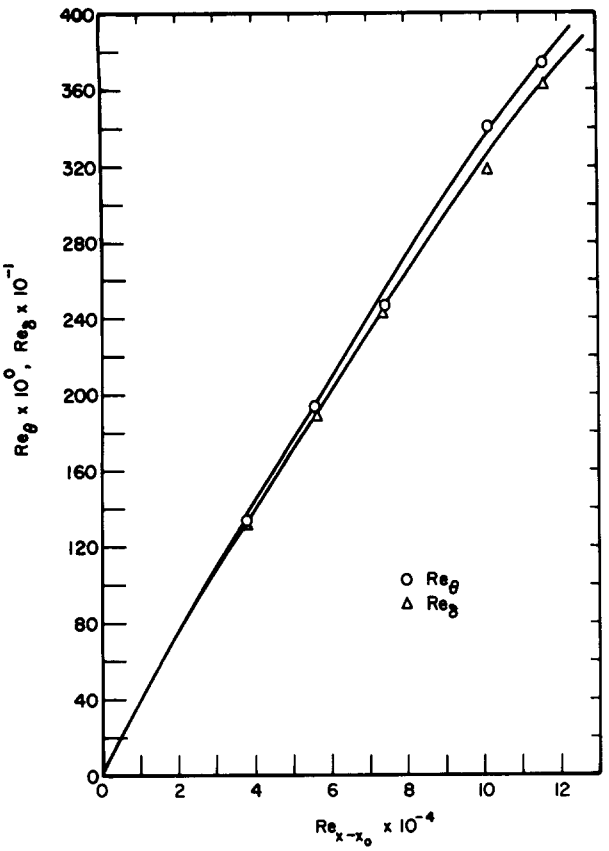

Fig. 4. Measured values of Re_θ and Re_δ.

Deposition results

As noted earlier, the objective of this study was to obtain experimental estimates of deposition under conditions of total ($\sigma_w = 1$) and partial ($\sigma_w < 1$) adhesion. In particular, the deposition information was to be obtained under controlled and well-defined turbulent conditions. The total sampling deposition area was 51.613 cm^2 as the plate was analyzed in strips 2 in. in the flow direction and 4 in. wide (the outer inch on each side was ignored).

The plate was exposed to the aerosol for 70 min per run. Each strip was then wiped with an absorbent tissue. A number of preliminary runs were conducted to insure the accuracy and reproducibility of the technique especially in the case of the fluorometric blank. Two plate surface conditions were tested with the relative humidity of the carrier gas constant at 58 %. The first set of experiments for $\tau_w = 1$ were run with the plate surface covered with a known volume of oil (Octoil S). Using an equation given by Perry [20] and data for Octoil S the surface tension force was found to be

0.1211 dynes for a 6.77 μm diameter particle. Because the calculated shearing stress at the plate surface was found to be several orders of magnitude less than the surface tension exhibited by the oil, it was assumed that any particle reaching the surface was retained by the oil film. The second experiment, for $\sigma < 1$, was run with a clean dry plate. Between each run the plate was thoroughly cleaned. Since all the particles reaching the wall are captured under conditions of $\sigma_w = 1$, the difference in the deposition fluxes for the conditions $\sigma_w = 1$ (condition 1) and $\sigma_w < 1$ (condition 2) yields the loss of particles from the plate under the dry surface condition. Mathematically, this gives

$$\sigma_{w1}\,\rho_{pw1}\left.\frac{F_w T_s}{m_p}\right|_1 - \sigma_{w2}\,\rho_{pw2}\left.\frac{F_w T_s}{m_p}\right|_2 = (1-\sigma_{w2})\,\rho_{pw2}\left.\frac{F_w T_s}{m_p}\right|_2$$

Since $\sigma_{w1} = 1$ the above reduces to

$$\rho_{pw1}\left.\frac{F_w T_s}{m_p}\right|_1 = \rho_{pw2}\left.\frac{F_w T_s}{m_p}\right|_2$$

Therefore, from eqn. (2)

$$\frac{J_1}{\sigma_{w1}} = \frac{J_2}{\sigma_{w2}}$$

But $\sigma_{w1} = 1$, hence

$$\sigma_{w2} = \frac{J_2}{J_1}$$

Table 1 gives the values of the mass flux, and σ_w for various plate positions under the two surface conditions. In assessing the magnitude of the computed values of σ_{w2} it should be recognized that the forces contributing to particle capture and retention under dry plate conditions include London—Van der Waal forces, hydrated layers on the aerosol surface and the surface roughness of the plate.

The averaged deposition results for the two experimental conditions considered are shown in Fig. 5. Figure 6 shows the variation of the attaching probabilities with downstream position. The trend for the plate follows the fluid behavior of the developing boundary layer. σ_{w2} is much higher on that part of the plate under the influence of the laminar free shear layer. The value decreases sharply at 2—4 in., due perhaps to reattachment and excessive rebounding. As the boundary layer grows and becomes more turbulent, mixing increases and so does the attachment probability. At x = 10—12 in., the fastest rate of growth is observed and the boundary layer then becomes more developed

TABLE 1

Plate position (inches)	J_1 $\left[\frac{\mu g}{cm^2\ s}\right] \times 10^6$	J_2 $\left[\frac{\mu g}{cm^2\ s}\right] \times 10^6$	$\sigma_{w2} = \frac{J_2}{J_1}$
0—2	4.225[a,b]	2.491[a,c]	0.5854
2—4	4.142	1.813	0.4377
4—6	3.734	2.353	0.6302
6—8	4.106	2.768	0.6741
8—10	4.428	3.091	0.6981
10—12	4.705	3.367	0.7156
12—14	4.982	3.506	0.7037
14—16	5.213	3.644	0.6990
16—18	5.397	3.713	0.6879
18—20	5.582	3.737	0.6695
20—22	5.674	3.759	0.6625
22—24	5.766	3.783	0.6561

[a] Average values.
[b] Oil-covered plate.
[c] Polished dry plate.

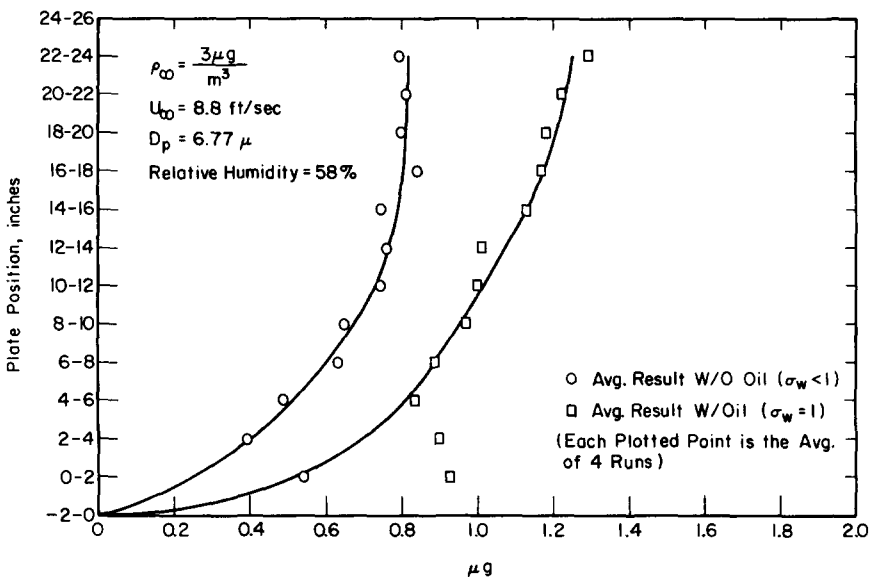

Fig. 5. Particle deposition distribution.

and turbulent with a decline in σ_w to relative constancy at x = 19 in. Of particular interest in the figure is the constancy of σ_w in a fully developed turbulent boundary layer (x = 19—24 in.). This lack of spatial dependency for σ_w will be particularly important for theoretical models dealing with fully developed turbulent boundary layers with deposition. It is hoped that the

results presented in this paper will be of use to researchers dealing with the deposition of particles in fully developed boundary layers.

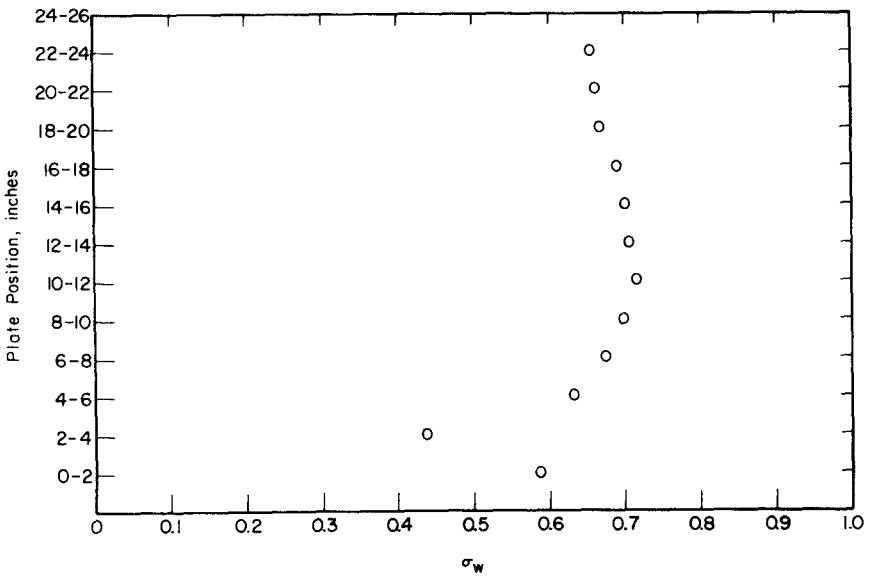

Fig. 6. Particle-attaching coefficient distribution.

Acknowledgement

Mr. Wedding was supported by a NSF RANN Grant No. GI—31605 while this research was being carried out. This support is gratefully acknowledged.

References

1 S.K. Friedlander, Deposition of Aerosol Particles from Turbulent Gases, Ph.D. Thesis, Univ. of Illinois, Urbana, Ill., 1954.
2 S.K. Friedlander and H.F. Johnstone, Ind. Eng. Chem., 49 (1957) 1151.
3 P.R. Owen, Int. J. Air Water Pollution, 3 (1960) 8.
4 C.W. Davies, Ann. Occup. Hyg., 8 (1965) 239.
5 C.W. Davies, Proc. Roy. Soc., Ser. A, London, 289 (1966) 235.
6 G.A. Sehmel, BNWL 578, Pacific Northwest Lab., Richmond, Washington, 1968.
7 G.A. Sehmel, J. Coll. Interface Sci., 37 (1971) 891.
8 S.L. Soo, Fluid Dynamics of Multiphase Systems, Blaisdell Publ. Co., Waltham, Mass., 1967.
9 S.L. Soo, Appl. Sci. Res., 21 (1969) 68.
10 S.L. Soo and S.K. Tung, Powder Technol., 6 (1972) 283.
11 S.L. Soo and L.W. Rodgers, Powder Technol., 5 (1971—72) 43.
12 S.L. Soo, Int. J. Multiphase Flow, 1 (1973) 89.
13 J.B. Wedding, Theory, Design and Characterization of an Aerosol Generation System Utilizing Ultrasonic Sound, M.S. Thesis, Univ. of Illinois, Urbana, Ill., 1972.

14 H.L. Green and W.R. Lane, Particle Clouds, Dusts, Smokes and Mists, E. and F.N. Spon Ltd., London, 1957.
15 W.D. Baines and E.A. Peterson, Trans. ASME, (July 1951) 467.
16 J.M. Robertson, A Turbulence Primer, Univ. of Illinois Engr. Exp. Sta. Circ. 79, 1963.
17 M. Hansen, Z. Angew. Math. Mech., 8, 2, 185.
18 J.M. Robertson, ASCE Mechanics Series, Monograph M-1, 1969, p. 14.
19 P.S. Klebanoff, Nat. Bur. Standards, NACA Rep. 1247, 1954.
20 J.H. Perry, Chemical Engineer's Handbook, McGraw-Hill, New York, 4th edn., 1963, pp. 3—215.